

Mutagenesis of nitrite reductase from *Pseudomonas aeruginosa*: tyrosine-10 in the c heme domain is not involved in catalysis

Francesca Cutruzzolà*, Marzia Arese, Sabrina Grasso, Andrea Bellelli, Maurizio Brunori

Dipartimento di Scienze Biochimiche 'A. Rossi Fanelli' and Centro di Biologia Molecolare del CNR, Università di Roma 'La Sapienza',
P.le A. Moro 5, 00185 Roma, Italy

Received 25 February 1997; revised version received 3 May 1997

Abstract In *Pseudomonas aeruginosa*, conversion of nitrite to NO in dissimilatory denitrification is catalyzed by the enzyme nitrite reductase (NiR), a homodimer containing a covalently bound c heme and a d₁ heme per subunit. We report the purification and characterization of the first single mutant of *P. aeruginosa* cd₁ NiR in which Tyr¹⁰ has been replaced by Phe; this amino acid was chosen as a possibly important residue in the catalytic mechanism of this enzyme based on the proposal (Fülöp, V., Moir, J.W.B., Ferguson, S.J. and Hajdu, J. (1995) Cell 81, 369–377) that the topologically homologous Tyr²⁵ plays a crucial role in controlling the activity of the cd₁ NiR from *Thiosphaera pantotropha*. Our results show that in *P. aeruginosa* NiR substitution of Tyr¹⁰ with Phe has no effect on the activity, optical spectroscopy and electron transfer kinetics of the enzyme, indicating that distal coordination of the Fe³⁺ of the d₁ heme is provided by different side-chains in different species.

© 1997 Federation of European Biochemical Societies.

Key words: Denitrification; Protein engineering; Electron transfer; Nitric oxide

1. Introduction

Nitrogen metabolism in the biosphere comprises several interconversion pathways carried out by different microorganisms. In dissimilatory denitrification, nitrates and nitrites are reduced to N₂ via gaseous metabolites, such as nitric oxide and nitrous oxide, whereas in the assimilatory pathway ammonia and amines are produced. The main biological role of dissimilatory denitrification is anaerobic respiration, although photorespiration and maintenance of redox balance are also important in some species. Organization and bioenergetics of electron transport chains involved in dissimilatory denitrification in *Paracoccus denitrificans*, *Escherichia coli* and photosynthetic bacteria, such as those from *Rhodobacter* sp., have been recently reviewed, in comparison to other species [1]. The best-known example of a denitrification chain is that from *P. denitrificans* where electron donors to ubiquinone are primarily NADH and succinate. The membrane-bound nitrate reductase receives electrons from the ubiquinol pool directly in an electron transfer process coupled to the formation of a transmembrane proton electrochemical gradient. Electrons are

then delivered from ubiquinol to the nitrite, nitric oxide and nitrous oxide reductases via the cytochrome *bc*₁ complex (also resulting in net proton translocation) and various periplasmic electron transport proteins.

The conversion of nitrite to nitric oxide is catalyzed by the periplasmic nitrite reductases (NiR) which are either copper- or heme-containing enzymes. Copper NiRs are usually homotrimers, with one type-I and one type-II copper bound per subunit [1]; heme NiRs are homodimers of two 60-kDa subunits, each containing one covalently bound c heme and one d₁ heme. The latter enzymes are capable of both monoelectronic reduction of NO₂[−] to NO and tetraelectronic reduction of O₂ to H₂O. Extensive spectroscopic and functional studies have been carried out on NiR from *Pseudomonas aeruginosa* (reviewed in [2]); the c heme domain has been shown to be the electron's entry site whereas conversion of substrates into products occurs at the level of the d₁ heme. The 3D structure of NiR from *P. aeruginosa* has been recently solved by X-ray diffraction (Cambillau, Tegoni et al., to be published); meanwhile, the high-resolution crystal structure of the oxidized cd₁ NiR from *Thiosphaera pantotropha* (a strain of *P. denitrificans*) has been published [3]. The atomic model shows that each subunit is organized in two structurally distinct domains: an N-terminal α-helical domain containing the c heme and a C-terminal eight-blade β-propeller domain with the d₁ heme-binding crevice. An unexpected ligand arrangement for the two redox centres was observed in the *T. pantotropha* structure: the oxidized c heme is a bis-histidinate (His¹⁷-His⁶⁹) coordination whereas the Fe³⁺ of the d₁ heme coordinates the nitrogen of His²⁰⁰ (proximal ligand) and the oxygen atom of Tyr²⁵ which belongs to the c heme-binding domain. The latter residue was proposed by Fülöp et al. [3] to play a key role in the mechanism of both nitrite and oxygen reduction by NiR. According to their scheme, during the catalytic cycle domain movement occurs, and Tyr²⁵ (which is not an axial ligand of the Fe²⁺ d₁ heme) swings in and out of the active site pocket, playing a crucial role in the displacement of the reaction product(s).

Whether this mechanism is generally valid for different cd₁ NiRs is, however, somewhat doubtful as already pointed out by Fülöp et al. [3]. As shown in Fig. 1, sequence comparison shows a reasonable degree of homology in the c heme domain; however, a substantial heterogeneity is found at the N-terminus where Tyr²⁵ is located in the *T. pantotropha* enzyme. The NiRs from *Pseudomonas stutzeri* and *Alcaligenes eutrophus* display a 20–30-amino-acid deletion at the N-terminus and, therefore, lack a Tyr in this region; on the other hand, in *P. aeruginosa* NiR, the shorter N-terminal tail contains a Tyr at position 10 which may or may not play the role assigned to Tyr²⁵ in *T. pantotropha*. In the crystal structure of *P. aeruginosa* NiR, Tyr¹⁰ is protruding into the d₁ heme pocket.

*Corresponding author. Fax: (39) (6) 444 0062.
E-mail: cutruzzola@axcasp.casur.it

Abbreviations: NiR, nitrite reductase; ET, electron transfer; PCR, polymerase chain reaction; 3D, three-dimensional; SVD, singular value decomposition

This paper is dedicated to our beloved friend Maria Chiara Silvestrini, prematurely deceased on 12 September 1996.

et but not at binding distance from the Fe^{3+} (Nurizzo et al., submitted).

In order to test the role of the N-terminal Tyr¹⁰ in *P. aeruginosa* cd_1 NiR we have produced, purified and characterized a site-directed mutant in which the residue has been replaced by Phe (Y10F). The optical spectrum, the nitrite reductase and oxidase activities, and the c-to- d_1 electron transfer rate of the Y10F mutant are unchanged compared to wild-type. These data show that Tyr at position 10 plays no role in the catalytic mechanism of *P. aeruginosa* NiR, and that probably functional role and direct Tyr coordination of the d_1 heme are peculiar to the NiR from *T. pantotropha* [3].

2. Materials and methods

2.1. Mutagenesis

Mutagenesis of Tyr¹⁰ was performed on the *nirS* gene previously isolated [4] by PCR methods [5]. In this paper, amino-acid numbering refers to the mature protein sequence whereas nucleotide numbering includes the 25-amino-acid signal sequence and the upstream region up to the *EcoRI* site already described [4]. Prior to mutagenesis, an *EcoRI*-*Apal* fragment containing *nirS* was subcloned from the plasmid pNMNR [6] in the vector Bluescript SkII⁺ (Stratagene) to eliminate non-unique restriction sites in the region downstream *nirS*, yielding the plasmid pBS-NR. Three different oligonucleotides were synthesized corresponding to (1) the 5' end of the *nirS* nucleotide sequence (5'-CGGCGCGAATTCCTCGGGAGTTCCTCGACGCAGC-CACCCCC-3'); (2) the region of the mutation (5'-GCCGCTGAG-CAATTCAGGGTGCCGC-3') and (3) a region around amino acid 42, ending with a unique *Bgl*II site (5'-GTAGATCTGCTGGCCTC-GTTGAACCTCG-3'). Oligonucleotide 2 also included a silent mutation introducing an extra *Bpl*I site to help selection of mutants. A first 113-bp fragment, synthesized by PCR using primers 1 and 2 and Vent DNA Polymerase (Biolabs) (annealing $t = 56^\circ\text{C}$), was used as a primer in a second PCR step for 7 cycles alone and then in combination with primer 3. The resulting 291-bp fragment, digested with *Bse*RI and *Bgl*II and purified, was subcloned in pBS-NR in place of the corresponding wild-type region. The mutant Y10F gene was first isolated by restriction analysis and then was completely sequenced in the region between the *Bse*RI and *Bgl*II sites (corresponding to that amplified by PCR) by the dideoxy method with Sequenase 2.0 Reagents (US Biochemicals). The *EcoRI*-*Apal* fragment containing the Y10F gene was then reintroduced in the expression vector pNM185 [7] together with the downstream region to obtain the expression construct pNM-Y10F.

2.2. Protein expression and purification

Expression in *Pseudomonas putida* PaW340 and purification of the wild-type and mutant protein was carried out as already described in [6], except that *m*-toluate induction was optimized, i.e. the inducer added at cell density = 0.9 (OD_{600}) and growth carried out for 18–20 h; under these conditions, the higher NiR expression vs. cell paste yield was obtained. Amino-acid sequence of the first 15 N-terminal residues was carried out on purified NiR Y10F loaded on a gas-phase sequencer (Applied Biosystems model 470A) equipped with a phenylthiohydantoin amino-acid derivatives analyser (model 120A).

In the *P. putida* expression system [6], the protein is synthesized with the c heme but no d_1 heme is present; this semi apo-NiR is then reconstituted in vitro with the d_1 heme. Spectrophotometric titrations of the wild-type and Y10F semi apo-NiR with the d_1 heme were carried out at 20°C in 50 mM sodium phosphate buffer pH 7.0 in order to determine heme-binding stoichiometry. Bulk reconstitution was then carried out by incubating the proteins at 15°C for 60 min in 50 mM sodium phosphate buffer at pH 7.0 with a 1.5 stoichiometric excess of d_1 heme; purification from excess-free heme was obtained by gel filtration on a Sephadex G-25 column.

2.3. Spectroscopic and functional characterization

Optical spectra were recorded using a Jasco V-550 spectrophotometer equipped with a thermostatted stirring cell holder. Oxidation of reduced *P. aeruginosa* cytochrome c551 [8] was followed at 551 nm at 25°C in 50 mM sodium phosphate buffer pH 7.0 as described in [9];

cytochrome c551 concentrations were 1–13 μM and NiR concentration was 20 nM, based on the d_1 heme extinction coefficient $\epsilon_{640} = 41 \text{ mM}^{-1} \text{ cm}^{-1}$ [2]. Each point used in the calculation of Michaelis-Menten parameters corresponds to the mean of two to three measurements.

Nitrite reductase activity was measured in anaerobiosis in a gas-tight cuvette using azurin from *P. aeruginosa* as electron donor as described in [10]. The reaction was initiated by addition of sodium nitrite to the azurin-NiR mixture and azurin oxidation was followed at 625 nm where the reduced form does not absorb.

The internal electron transfer rate from the c to the d_1 heme was measured in anaerobiosis by stopped flow using a TN6500 (Tracor Northern, Middleton, WI) multi-diode array spectrometer for multi wavelength detection. Reduced azurin (400 μM before mixing) in degassed buffer containing a slight excess of sodium dithionite and 1 mM CO, was mixed with oxidized NiR (8 μM before mixing). The time course of the reaction was followed by recording transmittance spectra in the wavelength range of 380–530 nm. Analysis of the experimental data has been described elsewhere [11]. Briefly, the transmittance spectra were converted to absorbance and sequentially arranged into a matrix (A) such that each column is a spectrum and each row a time course at single wavelength. Matrix A was then submitted to the singular value decomposition (SVD) [12], a procedure which yields the three matrices U, S and V such that

$$A = U \times S \times V^T$$

Each column of the matrix U represents the spectrum of one of the spectral components identified by the algorithm. The elements of the diagonal matrix S, the singular values, represent the relative weights of the corresponding U columns while the columns of the matrix V yield the time courses of each spectral component. The significant spectroscopic components, were identified from their singular value (S), their consistency as spectra (U) and their time course (V). The time course of the significant spectroscopic components was then fitted to the minimal mechanism, i.e. a sequence of three irreversible exponential steps, using standard non-linear least-squares minimization routines.

3. Results

Substitution of Tyr¹⁰ with Phe in the *nirS* gene from *P. aeruginosa* was obtained by site-directed mutagenesis using PCR [5]. This method was chosen in view of the high GC content of the *P. aeruginosa* genes which considerably lowers the efficiency of other procedures. The mutant gene Y10F,

Pden	QEQAAPPKDF	AAALEDHKTK	TDNRYEPLSD	NLAQODVAAL	GAPEGIPALS
TpanDF	AAALEDHKTK	TDNRYEPLSD	NLAQODVAAL	GAPEGVTALS
AeutATKAEPKA	EPKAAITPLT
PsaerKDDMK	AAEQYQGAAS	AV.....DPAHV	VRTNGAPDMS
PsstuAAAPZEMT
	51				100
Pden	DAQYNEANKI	YFERCAGCHG	VLRRGATGKA	LTPDL.....TR
Tpan	DAQYNEANKI	YFERCAGCHG	VLRRGATGKA	LTPDL.....TR
Aeut	AAEFDHARQI	YFERCAGCHG	VLRRGATGKS	LTPDI.....TR
Psaer	ESEFNEAKQI	YFQRCAGCHG	VLRRGATGKP	LTPDI.....TQ
Psstu	AEEKEASKQI	YFERCAGCHG	VLRRGATGKN	LEPHWSKTEA	DGKKTGGTL
	101				148
Pden	DLGFDYLQSF	ITYGSPACMP	NWGTSGELTA	EQVDLMANYL	LLDPAAPP
Tpan	DLGFDYLQSF	ITYGSPACMP	NWGTSGELSA	EQVDLMANYL	LLDPAAPP
Aeut	ARGTEYLKTF	IKYGSACMP	NWGTSGDLTD	PEVDLMARYI	QLDPTTTP
Psaer	QRCCQYLEAL	ITYGTPLGMP	NWGSSEGLSK	EQITLMAKYI	QHTPTQPP
Psstu	NLGTRKLENT	YAYTEGGMV	NYD.....DLITK	EEINMARIY	QHTPTDLP

Fig. 1. Sequence alignment of the c heme domain of NiRs from different sources: *P. aeruginosa* (Psaer), *P. stutzeri* (Psst), *P. denitrificans* (Pden), *A. eutrophus* (Aeut) and *T. pantotropha* (Tpan). Multiple sequence alignment was obtained using the PILEUP module of the GCG Software Package version 9.0 (Wisconsin, USA). Aminoacid identities are marked with asterisks, except for the conserved Tyr which is labelled by an empty circle. The heme attachment site Cys-X-X-Cys and the axial His, His and Met ligands are in bold.

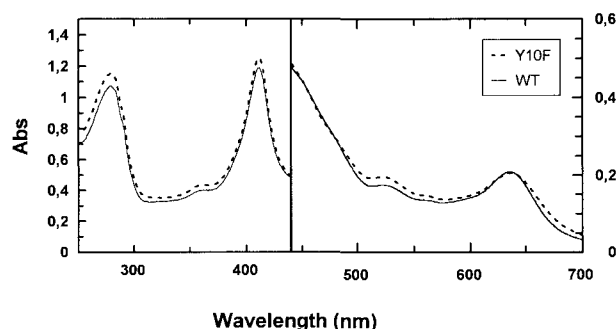


Fig. 2. Absorption spectra of the oxidized wild-type and Y10F mutant. The different Y scales used for the 250–440- and 440–700-nm intervals are shown on left and right panels. Protein concentration was 5 μ M in sodium phosphate 100 mM pH 7.0 and light path 1 cm. (NiR purified according to ref. [6] is obtained in the oxidized state and thus no oxidant was added.)

completely sequenced in the region of mutagenesis by PCR, was cloned in the expression vector pNM185 and the protein expressed and purified as described in Section 2. The yield of expression for Y10F was comparable to that of the wild-type protein [6]. The successful introduction of Phe at position 10 in the mature protein was also confirmed at the protein level

by determination of the amino-acid sequence for the first 15 residues.

The wild-type and Y10F apo-NiR were reconstituted *in vitro* with the d_1 heme and the spectra of the oxidized proteins between 260 and 700 nm are shown in Fig. 2. The typical absorption bands at 411 and 520 nm for the c heme and at 460 and 640 nm for the d_1 heme [2] were observed for both proteins, with no significant differences in position and intensity of the peaks.

To assess the role of Tyr¹⁰ in the physiological activity of cd_1 NiR, it is critical to measure the nitrite reductase activity. This reaction was studied in anaerobiosis using reduced azurin from *P. aeruginosa* as an electron donor at a NaNO_2 concentration well above the K_M and at two different pH values (6.2 and 7.0)[10]. Typical results are depicted in Fig. 3 for the native, the wild-type and the Y10F single mutant NiRs: the time course of azurin oxidation at pH 6.2 and 27°C is almost identical for the three proteins. Under these conditions, the turnover number is 67 mol azurin/mol \times min for wild-type and 60 mol azurin/mol \times min for Y10F (S.D. \pm 10%). K_M for nitrite is also unchanged ($K_M = 35 \pm 10 \mu\text{M}$). It is reported in the literature that an increase in pH towards neutrality inhibits the *P. aeruginosa* enzyme [10,13], probably as a consequence of the ionization of some residue critical for catalysis. To rule

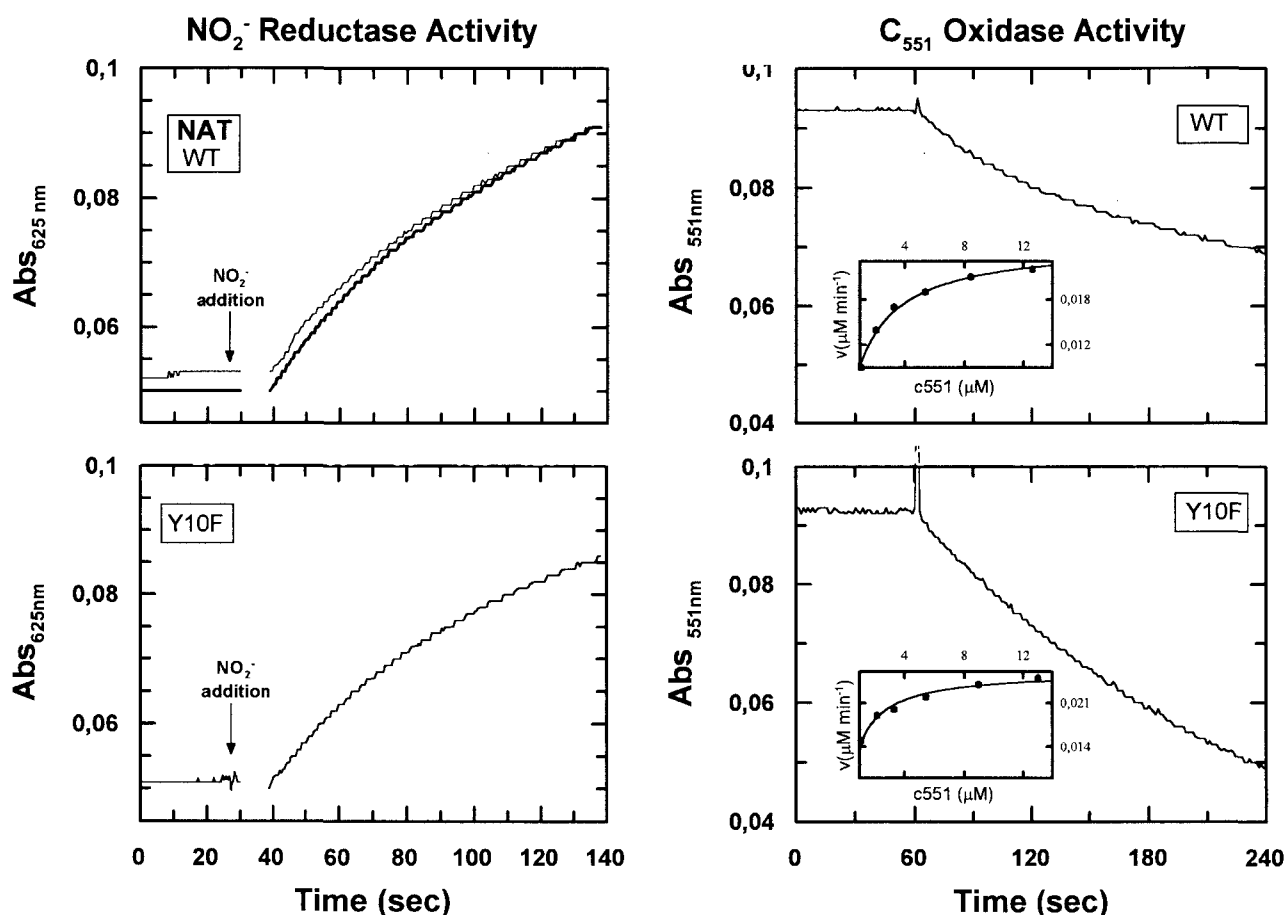
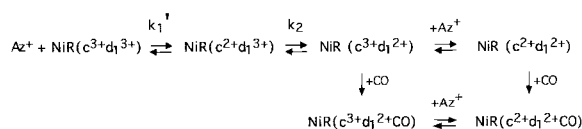


Fig. 3. Nitrite reductase (left panels) and cytochrome oxidase (right panels) activity of native (thick line), wild-type and Y10F NiRs. Left panels: concentrations were: azurin 40 μ M, sodium nitrite 600 μ M and NiR 0.1 μ M at 27°C in 50 mM sodium phosphate buffer at pH 6.2. The time of nitrite addition is indicated by the arrow. Right panels: experimental conditions were 100 mM sodium phosphate buffer at pH 7.0, 25°C and NiR concentration 15 nM; the trace correspond to a cytochrome $c551$ concentration of 3 μ M. The insets show the rates (●) measured at different substrate concentrations, fitted with a Michaelis-Menten equation.

out the involvement of Tyr¹⁰ in this inhibition, the same experiment was repeated at pH 7.0 (not shown): as expected, a lower rate was measured but no significant difference between the wild-type and Y10F NiRs was observed.

The ability of wild-type and Y10F NiRs to catalyze the oxidation of cytochrome *c*551, the physiological electron donor in *P. aeruginosa*, was assessed at pH 7.0 and 25°C. Fig. 3 shows the time course of this reaction for both NiRs at a single cytochrome *c*551 concentration. This reaction was shown to be complex also for the native enzyme [9] in that two different K_M values were observed at low and very high cytochrome *c*551 concentrations: our analysis of the observed rates obtained at low concentration yielded values of K_M and c.c.a. (catalytic centre activity) of 1.77 μM and 35 min^{-1} for the wild-type and of 0.84 μM and 36 min^{-1} (S.D. $\pm 10\%$ for all values) for the mutant Y10F, in good agreement with those previously published for the native enzyme [9].

As an additional test to highlight possible differences in the electron transfer kinetics between wild-type and Y10F NiRs we have measured by stopped flow the time course of reduction in the reaction of oxidized NiR with excess reduced azurin [14]. When reduced azurin in the presence of traces of sodium dithionite and 1 mM CO is mixed with oxidized NiR, the following reactions take place (see Scheme 1). The



Scheme 1.

presence of a large excess of both reduced azurin and CO drives the set of reactions (essentially irreversibly) to the right. Electron transfer from azurin to c heme and binding of CO to reduced d₁ heme are both very fast (pseudo first order for CO, $k_{\text{on}} = 500 \text{ s}^{-1}$ under these conditions) [14]. Fig. 4 shows the difference spectra (panels A and B) and the observed time courses (panels C and D) of the corresponding species as obtained from data analysis (see Section 2). The time courses of the reaction of native, wild-type and Y10F NiRs are very similar; this can be seen by observation at individual wavelengths (460 and 420 nm) or from observation of the two major spectroscopic SVD components (V columns 1 and 2). The three data set were minimized together with a global fitting procedure which yielded the two significant rate constants in Scheme 1. The first process, characterized by the higher rate constant ($k_1' = 28 \text{ s}^{-1}$), is attributed to the reduction of the c heme while the second process ($k_2 = 0.81 \text{ s}^{-1}$)

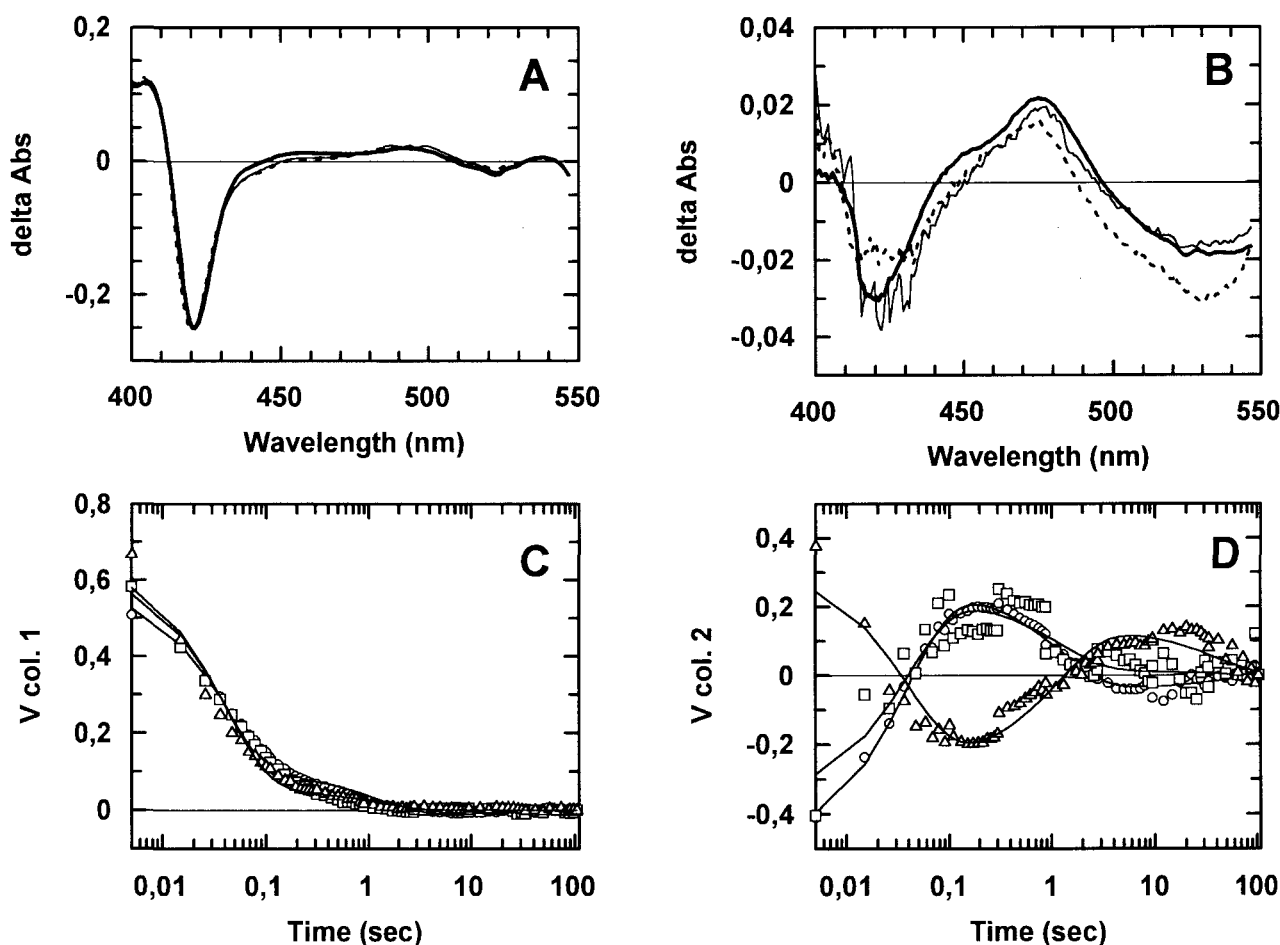


Fig. 4. Kinetics of electron transfer: difference spectra of NiR (c^3+d_1^3+) minus NiR (c^2+d_1^3+) (panel A) and NiR (c^2+d_1^3+) minus NiR ($\text{c}^2+\text{d}_1^2+\text{CO}$) (panel B) as obtained from SVD of stopped-flow spectroscopy. In both panels, thin and dotted lines indicate the spectrum of the wild-type and Y10F species, respectively, and bold line the spectrum of native NiR; the differences are taken to be within experimental errors. The time courses of the main spectroscopic components detected by SVD are shown in panels C and D; native NiR (\circ), wild-type (\square) and Y10F (\triangle) recombinant NiRs. The continuous lines represent the best fits according to Scheme 1.

corresponds to the internal electron transfer from the c to the d₁ heme, in agreement with [14]. As evident from Fig. 4D, a third very slow kinetic process ($k = 0.02 \text{ s}^{-1}$) is observed as an evolution of the second larger spectroscopic component detected by the SVD; this corresponds to a very small absorbance transition, tentatively assigned to a structural re-arrangement of the CO-bound d₁ heme.

4. Discussion

Understanding the catalytic mechanism of cd₁ NiR has several interesting implications. This enzyme is capable to catalyze efficiently both the one electron reduction of NO₂[−] to NO and the four electron reduction of O₂ to H₂O. Moreover, nitrite reduction (the enzyme's physiological activity) yields NO which is the substrate of NO reductase, the next enzyme in the denitrification chain; this reaction is intrinsically interesting since the affinity of NO for ferrous iron is known to be high [15] and NO has been involved in a number of key signalling processes in eukaryotes [16]. Heme-containing NiRs are also very interesting from an evolutionary viewpoint since they appear to use different catalytic strategies although belonging to a family in which sequence conservation is fairly high. The structures of cd₁ NiRs from *T. pantotropha* [3] and *P. aeruginosa* (Nurizzo et al., submitted) are now available. Mutagenesis studies have become feasible in our group since recombinant *P. aeruginosa* cd₁ NiR was expressed [6]; the latter enzyme was successfully used to obtain NiR reconstituted with a photoexcitable porphyrin [17].

In this paper, we present the characterization of the first single mutant of *P. aeruginosa* cd₁ NiR in which Tyr¹⁰ has been replaced with Phe (Y10F). As outlined in Section 1, this residue was chosen as a possible candidate to play a role in the catalytic mechanism of the NiRs based on the proposal by Fülöp et al. for Tyr²⁵ in the cd₁ NiR from *T. pantotropha* [3]. In the latter NiR, Tyr²⁵ is coordinated to the d₁ heme in the oxidized form; if this was the case also for the *P. aeruginosa* NiR, significant spectroscopic changes in the d₁ heme absorption bands may have been expected. Data in Fig. 2 show that this is not observed and the spectrum of the oxidized form of the Y10F mutant is still consistent with an hexacoordinate d₁ heme [18].

The nitrite reductase and oxidase activities of the mutant Y10F NiR are essentially retained compared to wild-type NiR (Fig. 3). The difference in K_M value for cytochrome c551 is difficult to account for but may be due to a different conformation of the N-terminal domain containing the mutation. More importantly, the physiological nitrite reductase activity was shown to be unchanged in the Y10F enzyme, and its pH dependence similar to that previously shown for the native enzyme [10,13].

A peculiarity of the cd₁ NiR is the slow internal ET rate from the c to the d₁ heme within one monomer [14]. From the model of cd₁ NiR from *T. pantotropha*, the shortest edge to edge distance between the c and d₁ heme is 11 Å, too short to be compatible with the low c → d₁ ET rate constant ($k = 1 \text{ s}^{-1}$) ([14] and this work). A redox-dependent coordination change during catalysis (and, thus, a higher reorganization energy), possibly correlated with domain movement and coordination of Tyr²⁵, may have been postulated to account for such a low rate. If Tyr¹⁰ in *P. aeruginosa* NiR was directly involved in

such a change in coordination, mutation to Phe should have affected the c → d₁ ET rate. However, such an effect was not observed, indicating that the hexacoordinated state of the d₁ heme in the ferric derivative does not depend directly on Tyr¹⁰ and should involve another distal ligand (probably, a hydroxyl ion) intercalated between Tyr¹⁰ OH and the d₁ heme iron.

In conclusion, the results presented above show that substitution of Tyr¹⁰ with Phe in *P. aeruginosa* cd₁ NiR does not alter significantly the spectroscopic properties nor the activity of the enzyme; therefore, Tyr¹⁰ is not playing the same crucial role envisaged for Tyr²⁵ in *T. pantotropha* NiR [3]. The possibility still exists, however, that in *P. aeruginosa* NiR Tyr¹⁰ (and maybe Phe) exerts a 'second-sphere' influence by stabilizing a side-chain (or a ligand) important for catalysis; its replacement may, therefore, have more subtle consequences than the 'all-or-none' effect that we have excluded with the present work. To further understand the mechanism of *P. aeruginosa* cd₁ NiR, the crystal structure of the Y10F mutant as well as other mutations at residues possibly involved in ET, catalysis and release of NO will be determined.

Acknowledgements: We express our thanks to Dr. M.E. Schininà and Professor D. Barra (University of Rome 'La Sapienza', Italy) for N-terminal sequence, Dr. C. Cambillau (AFMB, CNRS Marseille, France) for the opportunity to quote structural data prior to publication, and Dr. E. Henry (NIH, Bethesda, MD) for advice in data handling. Grants from the European Union (Contract BIO4-CT96-0281) and from MURST (40% Liveprotein) are gratefully acknowledged.

References

- [1] Berks, B.C., Ferguson, S.J., Moir, J.W.B. and Richardson, D.J. (1995) *Biochim. Biophys. Acta* 1232, 97–173.
- [2] Silvestrini, M.C., Falcinelli, S., Ciabatti, I., Cutruzzolà, F. and Brunori, M. (1994) *Biochimie* 76, 641–654.
- [3] Fülöp, V., Moir, J.W.B., Ferguson, S.J. and Hajdu, J. (1995) *Cell* 81, 369–377.
- [4] Silvestrini, M.C., Galeotti, C.L., Gervais, M., Schininà, E., Barra, D., Bossa, F. and Brunori, M. (1989) *FEBS Lett.* 254, 33–38.
- [5] Zhao, L.J., Zhang, Q.X. and Padmanabhan, R. (1993) *Methods Enzymol.* 217, 218–227.
- [6] Silvestrini, M.C., Cutruzzolà, F., D'Alessandro, R., Brunori, M., Fochesato, N. and Zennaro, E. (1992) *Biochem. J.* 285, 661–666.
- [7] Mermoud, N., Ramos, J.L., Lehrbach, P.R. and Timmis, K. (1986) *J. Bacteriol.* 167, 447–454.
- [8] Cutruzzolà, F., Ciabatti, I., Rolli, G., Falcinelli, S., Arese, M., Ranghino, G., Anselmino, A., Zennaro, E. and Silvestrini, M.C. (1997) *Biochem. J.* 322, 35–42.
- [9] Tordi, M.G., Silvestrini, M.C., Colosimo, A., Tuttobello, L. and Brunori, M. (1985) *Biochem. J.* 230, 797–805.
- [10] Silvestrini, M.C., Colosimo, A., Brunori, M., Walsh, T.A., Barber, D. and Greenwood, C. (1979) *Biochem. J.* 183, 701–709.
- [11] Antonini, G., Bellelli, A., Brunori, M. and Falcioni, G. (1996) *Biochem. J.* 314, 533–540.
- [12] Henry, E.R. and Hofrichter, J. (1992) *Methods Enzymol.* 210, 129–192.
- [13] Silvestrini, M.C., Tordi, M.G., Musci, G. and Brunori, M. (1990) *J. Biol. Chem.* 265, 11783–11787.
- [14] Parr, S.R., Barber, D., Greenwood, C. and Brunori, M. (1977) *Biochem. J.* 167, 447–455.
- [15] Traylor, T.G. and Sharma, V.S. (1992) *Biochemistry* 31, 2847–2849.
- [16] Bredt, D.S. and Snyder, S.H. (1994) *Annu. Rev. Biochem.* 63, 175–195.
- [17] Bellelli, A., Brzezinski, P., Arese, M., Cutruzzolà, F., Silvestrini, M.C. and Brunori, M. (1996) *Biochem. J.* 319, 407–410.
- [18] Walsh, T.A., Johnson, M.K., Greenwood, C., Barber, D., Springall, J.P. and Thomson, A.J. (1979) *Biochem. J.* 177, 29–39.